– Cover Page –

Manuscript entitled:

Comparison of Lightning Protection Performance of Carbon/Epoxy Laminates with a Non-metallic Outer Layer

Submitted to:

Journal of Reinforced Plastics and Composites

Authored by:

Juhyeong Lee,[1*] Thomas E. Lacy Jr.,[2] Charles U. Pittman Jr.,[3] Michael S. Mazzola[4]

1. Advanced Composites Collaboration for Innovation & Science (ACCIS), Queens Building, University Walk, Bristol BS8 1TR, UK
2. Department of Mechanical Engineering, Texas A&M University, MEOB 429, College Station, TX 77843-3123, USA
3. Department of Chemistry, Mississippi State University, Mississippi State, MS 39762, USA
4. Department of Electrical and Computer Engineering, University of North Carolina at Charlotte, Charlotte, NC 28223, USA

Keywords: lightning damage prediction, non-metallic lightning protection system, finite element parametric study

* Corresponding author

Juhyeong Lee PhD

Research Associate
Advanced Composites Collaboration for Innovation and Science (ACCIS)
Department of Aerospace Engineering
Queens Building
University of Bristol
University Walk, Bristol BS8 1TR, UK
Email: Juhyeong.Lee@bristol.ac.uk

Abstract

This study shows how a lightning protection layer can be designed to effectively mitigate lightning damage in underlying composite structures. A parametric study was performed to characterize critical lightning protection layer properties that improve composite lightning damage resistance. Simulated 50 kA and 200 kA lightning strikes to pitch-based carbon fiber paper (PCFP) protected-AS4/3506 carbon/epoxy composites were considered in this study. The lightning protection characteristics of various PCFP outer layers were assessed by varying in-plane and through-thickness properties: electrical and thermal conductivities, and electrical and thermal gap conductances. The predicted matrix decomposition in the outermost AS4/3506 ply was significantly reduced by increasing the PCFP in-plane electrical conductivity. While predicted lightning damage decreased slightly with a decrease in thermal gap conductance, varying the electrical gap conductance and the in-plane and through-thickness thermal conductivities did not significantly affect damage development. Among various PCFP properties, the PCFP in-plane electrical conductivity was the most critical factor in reducing thermal damage development (thus, protecting the underlying AS4/3506 laminate). This parametric study demonstrates that it may be possible to tailor lightweight non-metallic lightning protection layers as an effective alternative to traditional metallic projection layers.

Introduction

Carbon fiber-reinforced polymer (CFRP) composites are becoming more widely used in high-performance aerospace applications due to their 1) excellent strength-to-weight ratios creating higher fuel efficiency, 2) design flexibility leading to easier fabrication of complex geometry parts,

and 3) high corrosion resistance that can withstand harsher environments compared to traditional aerospace-grade metal alloys [1].

Lightning is a naturally occurring, high voltage, high current, transient electrical discharge between two charged regions with opposite polarities [2]. The complex physics and the probabilistic nature of lightning renders an aircraft composite exterior skin surface susceptible to a lightning strike. A lightning strike can induce severe damage to aircraft structural components, essential electrical systems, and fuel tanks [3-6]. In contrast to traditional aerospace-grade metal alloys (aluminum, titanium, and magnesium, etc.), CFRP composites cannot efficiently distribute electrical currents due to their relatively low electrical conductivities; the severity of lightning damage generally decreases as a given material's electrical conductivity increases [7]. Lower electrical conductivity materials tend to absorb more electrical energy during lightning strikes due to increased Joule (resistive) heating. This raises serious concerns about using CFRP composites at critical aircraft locations susceptible to lightning strikes.

Conventional lightning strike protection systems are fabricated primarily from highly conductive aluminum or copper [8-10]. The use of dense metallic lightning protection layers somewhat offsets the benefits of using lightweight CFRP composites for aircraft structural applications. Arguably, CFRP composites should be designed with high electrical conductivities that enable them to withstand lightning currents with minimal damage [10, 11]. One possible approach to mitigate lightning damage is to bond highly conductive outer protection layers (i.e., metallic mesh/foil, carbon fiber (CF) paper, carbon nanofiber (CNF), or carbon nanotube (CNT) films, graphene sheets, buckypaper [8-10, 12-14]) to CFRP composites. Transversely isotropic carbon-based protection layers can be made of two-dimensional (2-D), randomly oriented CFs, CNFs, CNTs, or graphene nanoplatelets. A few lightning strike finite element (FE) models

have been developed to characterize lightning-induced thermal damage development in carbon/epoxy composites protected with *isotropic* pitch-based carbon fiber paper (PCFP) layer [15, 16] or buckypaper [17]. The use of an isotropic material assumption may be inappropriate, since lightning current flow is strongly governed by both the in-plane and through-thickness conductivities of the protection layer.

This study assesses the effect of varying lightning protection layer electrical and thermal properties on thermal damage development in an underlying composite. Here "thermal damage" primarily is associated with matrix decomposition. A FE-based parametric study was performed on pitch-based carbon fiber paper (PCFP) protected-AS4/3506 carbon/epoxy composites subjected to 50 kA peak lightning currents. Seventeen different nonlinear coupled electrical-thermal and transient heat transfer simulations were performed to assess epoxy matrix decomposition in 9-ply AS4/3506 composites ($[+45/-45/0_2/90/0_2/-45/+45]$, ply thickness = 0.2 mm) which contain a PCFP outer layer. The PCFP in-plane and through-thickness electrical/thermal conductivities and electrical/thermal gap conductances were varied. One goal of this work is to identify the optimal combination of PCFP and interfacial properties that most effectively reduce lightning thermal damage development.

FE Model for Matrix Decomposition Prediction

The lightning strike damage prediction FE models [15, 16] were previously developed to successfully predict lightning thermal damage (matrix decomposition, fiber sublimation/ablation) to AS4/3506 carbon/epoxy composites. In essence, electrical current-induced matrix decomposition and corresponding composite property changes were predicted based on the highest

local temperature reached during the analyses. This FE model is summarized as follows. See [15, 16] for a complete description of the modelling and analysis procedures.

AS4/3506 Carbon/Epoxy Composite and PCFP Properties

Temperature-dependent AS/3506 carbon/epoxy composite properties used in the simulations were obtained from the literature [18-24] (Table 1). The epoxy matrix was assumed to decompose over the temperature range 300-500˚C [15, 16]. The composite latent heat of *fusion* (4.8×10^3 kJ/kg) [22] associated with matrix decomposition was defined only between 300-500˚C. The fibers and matrix residue/char were assumed to begin ablating when the local temperature exceeded the fiber sublimation temperature (3,316˚C, [23]) and were fully abated at the critical sublimation temperature (3,367˚C, [24]). Once fiber sublimation began to occur (3,316˚C), the composite conductivities were assumed to be isotropic as a consequence of irreversible char/residue formation from the matrix. The composite latent heat of *vaporization* was 4.3×10^4 kJ/kg [22] absorbed between 3,316-3,367˚C.

Table 1. AS4/3506 carbon/epoxy material properties [18-21]

Temp.	Density[a]	Specific Heat[a]	Thermal Conductivity[a]			Electrical Conductivity[b]		
			Longi.	Trans.	Thick.	Longi.	Trans.	Thick.
(˚C),	(Kg/mm^3)	(J/kg/K)	(W/mm/K)	(W/mm/K)	(W/mm/K)	(S/mm)	(S/mm)	(S/mm)
11	1.5×10^{-6}	1,065	4.7×10^{-2}	6.8×10^{-4}	6.8×10^{-4}	35.97	1.15×10^{-3}	3.9×10^{-6}
350	1.5×10^{-6}	2,100	2.5×10^{-2}	3.7×10^{-4}	3.7×10^{-4}	35.97	1.15×10^{-3}	3.9×10^{-6}
510	1.1×10^{-6}	2,100	1.5×10^{-2}	1.8×10^{-4}	1.8×10^{-4}	35.97	2	2
1,000	1.1×10^{-6}	5,750	1.2×10^{-2}	1.3×10^{-4}	1.3×10^{-4}	35.97	2	2
3,316	1.1×10^{-6}	5,875	1.0×10^{-4}	1.0×10^{-4}	1.0×10^{-4}	35.97	2	2
3,367	1.1×10^{-6c}	5,875[c]	1.0×10^{-4c}	1.0×10^{-4c}	1.0×10^{-4c}	1[c]	1[c]	1.0×10^{-6c}

[a]Refs. [18, 19], [b]Refs. [20, 21].
[c]Properties determined by the extrapolation of the empirical data over the temperature range (25-3316˚C).

Transversely isotropic PCFP is comprised of short pitch carbon fibers (PCFs) that are 2-D, randomly-oriented in the in-plane directions. While in-plane properties of a PCFP layer have been reasonably well characterized by the manufacturer [25], its through-thickness properties are not well understood due to the difficulty of testing. Thus, several major assumptions about the PCFP have historically been made: (*i*) both the thermal and electrical conductivity tensors were assumed to be *isotropic*, *ii*) the thermal conductivities were obtained by averaging the axial and radial conductivities of a single PCF, *iii*) the in-plane electrical conductivity corresponded to the in-plane conductivity for DONACARBO PCFP (Osaka Gas Chemicals S-259 grade [25]) , and *iv*) the PCFP specific heats were assumed to be those of bulk graphite. These assumed properties [25-29] (Table 2) are considered as the "baseline" PCFP properties in this study. In addition, the "baseline" electrical conductance of 2.5×10^7 S/m^2 [27] and thermal gap conductance of 500 W/m^2 K [29] were assumed between the PCFP and AS4/3506 composite. A more detailed description of PCFP properties was presented previously [15, 16]. In this study, numerical simulations were performed where the baseline PCFP in-plane and through-thickness electrical/thermal conductivities and electrical/thermal gap conductances were each varied by an order-of-magnitude to assess their effects on lightning damage development.

Table 2. Baseline PCFP material properties [25, 26, 28]

Temp. (˚C)	Density[a] (kg/mm^3)	Specific Heat[b] (kg/mm^3)	Electrical Conductivity[c] (S/mm)	Thermal Conductivity[a] (W/mm/K)
25	1.6×10^{-6}	803	11.1	0.20
500	1.6×10^{-6}	1,598	11.1	0.19
1,000	1.6×10^{-6}	1,947	11.1	0.17
1,500	1.6×10^{-6}	2,096	11.1	0.16
2,000	1.6×10^{-6}	2,170	11.1	0.15
3,000	1.6×10^{-6}	2,234	11.1	0.12
3,316	1.6×10^{-6}	2,245	11.1	0.11
3,367	1.6×10^{-6}[d]	2,245[d]	11.1[d]	0.10[d]
4,000	1.6×10^{-6}[d]	2,245[d]	11.1[d]	0.10[d]

[a]Ref. [25], [b]Ref. [26], and [c]Ref. [28].

[d]Properties extrapolated from the empirical data over the temperature range (25-3316˚C).

Because of its 2-D random distribution of PCFs, a typical PCFP displays much higher electrical and thermal conductivities in the in-plane directions than in the through-thickness direction; therefore, the previously mentioned isotropic material assumption is physically unrealistic. The distribution of electrical current flow and heat transfer through an idealized isotropic layer may be profoundly different from those of a more realistic transversely isotropic layer. For instance, protection layers with both high in-plane and through-thickness electrical conductivities lead to lower internal thermal damage development [15, 16, 30].

A total of 17 numerical simulations of 50 kA peak current lightning strikes to PCFP-protected AS4/3506 laminates was performed. In the first simulation, the assumed baseline isotropic PCFP properties (Table 2) were employed. In the remaining 16 simulations, the baseline in-plane and through-thickness electrical conductivities, in-plane and through-thickness thermal conductivities, electrical gap conductance, and thermal gap conductance were each successively increased or decreased by an order-of-magnitude. Table 3 contains a summary of the factors used to scale the

material properties in each of the 17 simulations. For example, in Case 5 both the in-plane and through-thickness electrical conductivities are 10 times greater than the baseline values (defined in Table 2), while the other properties remain unchanged. In Cases 1-6, the in-plane and transverse electrical conductivities are independently scaled by factors of 1/10 and 10 from the baseline values (Table 2), while holding the thermal conductivities and gap conductances fixed. In Cases 7-12, the in-plane and transverse thermal conductivities are scaled in a similar fashion. Lastly, Cases 13-14 and 15-16 correspond to the cases where the electrical gap conductance and thermal gap conductance, respectively, are scaled accordingly. These simulations can be used to assess the effect of protection layer anisotropy and interfacial properties on lightning damage development.

Table 3. Sixteen sets of PCFP properties used in the parametric study

Property Set	Electrical Conductivity		Electrical Gap Conductance	Thermal Conductivity		Thermal Gap Conductance
	In-plane	Through-Thickness		In-plane	Through-Thickness	
Baseline	× 1	× 1	× 1	× 1	× 1	× 1
Case 1	× 10	× 1	× 1	× 1	× 1	× 1
Case 2	× 0.1	× 1	× 1	× 1	× 1	× 1
Case 3	× 1	× 10	× 1	× 1	× 1	× 1
Case 4	× 1	× 0.1	× 1	× 1	× 1	× 1
Case 5	× 10	× 10	× 1	× 1	× 1	× 1
Case 6	× 0.1	× 0.1	× 1	× 1	× 1	× 1
Case 7	× 1	× 1	× 1	× 10	× 1	× 1
Case 8	× 1	× 1	× 1	× 0.1	× 1	× 1
Case 9	× 1	× 1	× 1	× 1	× 10	× 1
Case 10	× 1	× 1	× 1	× 1	× 0.1	× 1
Case 11	× 1	× 1	× 1	× 10	× 10	× 1
Case 12	× 1	× 1	× 1	× 0.1	× 0.1	× 1
Case 13	× 1	× 1	× 10	× 1	× 1	× 1
Case 14	× 1	× 1	× 0.1	× 1	× 1	× 1
Case 15	× 1	× 1	× 1	× 1	× 1	× 10
Case 16	× 1	× 1	× 1	× 1	× 1	× 0.1

*Sixteen sets of PCFP properties are obtained by multiplying the baseline properties (Table 2) by the numbers indicated in each row of Table 3.

FE Lightning Strike Modeling and Boundary Conditions

Following the modelling procedure and mesh-sensitivity analysis established in [15, 16], FE models were developed for 150×150 mm^2 AS4/3506 carbon/epoxy laminates with a 0.5 mm thick PCFP protection layer (Fig. 1). The AS4/3506 layup was $[+45/-45/0_2/90/0_2/-45/+45]$ with 0.2 mm ply thickness. The uniform FE mesh consisted of eight-node linear coupled electrical-thermal continuum elements with in-plane dimensions, 2.5×2.5 mm^2. Each ply was discretized using a single element through its thickness. ABAQUS surface-to-surface general contact [31] was used to define the electrical and thermal gap conductances between the PCFP outer layer and underlying composite.

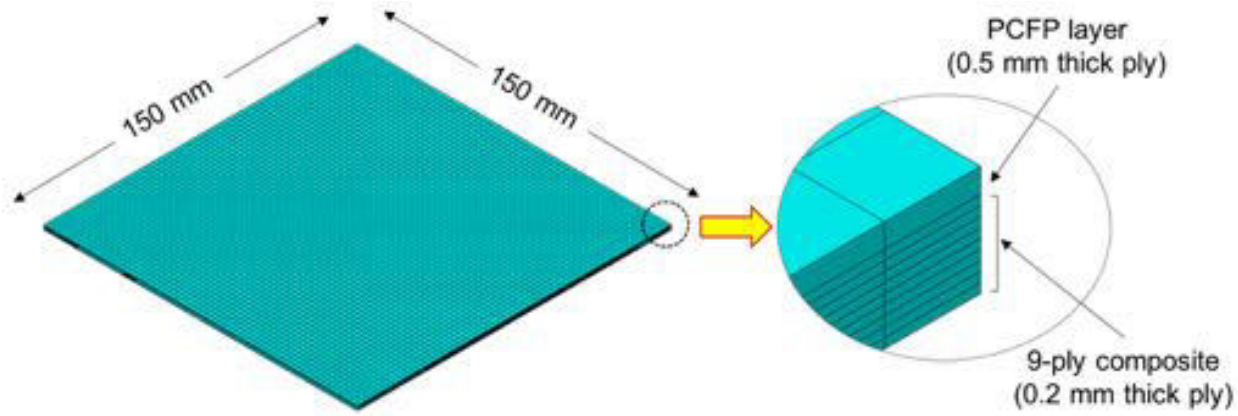

Figure 1. Lightning strike FE model geometry and discretization.

The lightning strike FE models [15, 16] were used to perform two-step transient analyses: *i*) a coupled electrical-thermal analysis to determine the local temperature rise due to Joule heating (resistive) heating in the first 30 μs after lightning attachment followed by *ii*) a *transient* heat transfer analysis for 10 s. In a coupled electrical-thermal analysis, Joule heating occurs *instantaneously* with current passage and heat transfer is almost negligible in this short time span. In contrast, after 10 s the heat transfer has occurred to the degree that also creates damage to the

composite. Each analysis requires assigning either electrical or thermal boundary conditions to calculate the electrical potential, current density, and temperature distributions. The boundary conditions implemented in this FE parametric study were consistent with those used in our recent artificial lightning strike tests (Fig. 2) [32, 33]. In the presence of electrical current (during the coupled electrical-thermal analysis), zero electrical potentials for grounding the current were imposed on all four edges of the simulated composites. Thermal boundary conditions were only applied on the exposed top surface of the PCFP outer layer: *i*) radiation boundary conditions (surface emissivity, 0.85 [18]; ambient surrounding temperature, 25˚C) were employed during all simulations, and *ii*) convection boundary conditions (convection coefficient, 200 $W/m^2/K$ [34]) were additionally assigned during the subsequent heat transfer analyses to account for considerable thermal advection. The electrical and thermal boundary conditions used in two-step transient analyses are summarized in Fig. 3. Note that the electrical potential boundary condition was not defined in a transient heat transfer analysis due to the lack of electrical current.

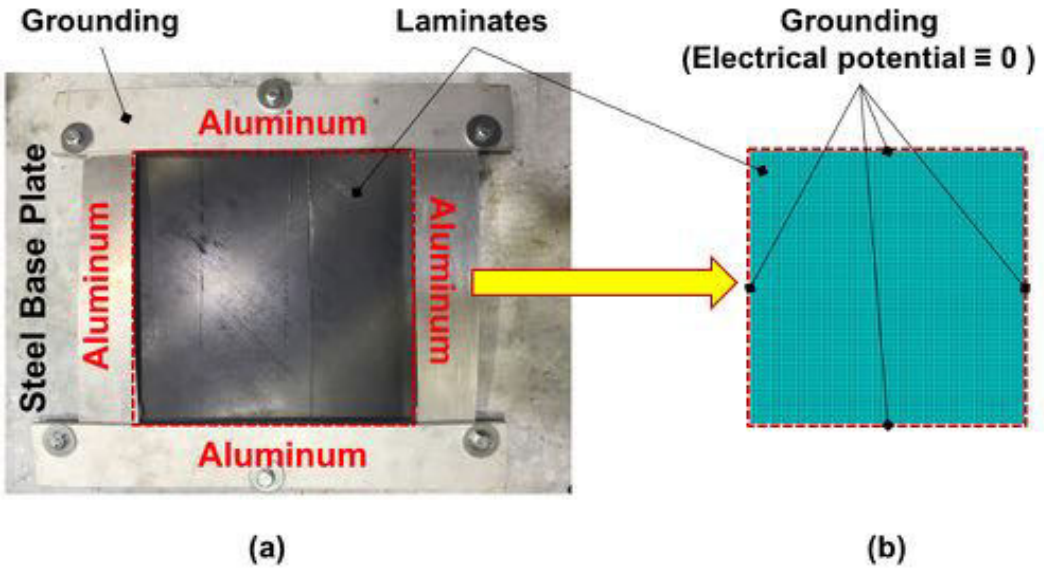

Figure 2. (a) Experimental lightning test specimen and (b) corresponding composite FE representation of electrical grounding conditions [32, 33].

5

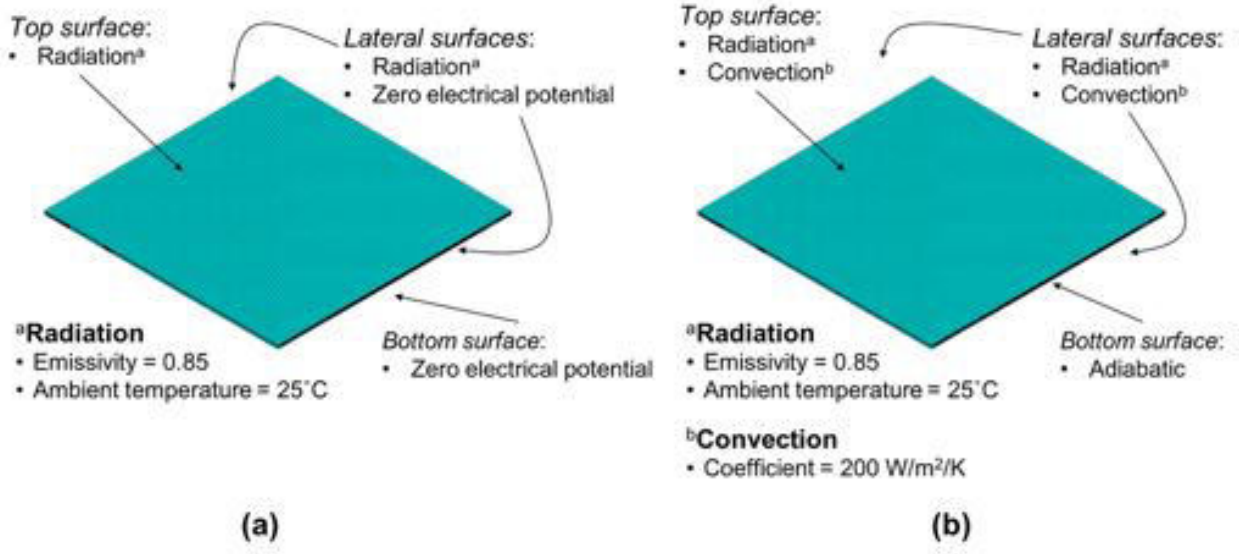

Figure 3.Electrical and thermal boundary conditions defined in (a) coupled thermal-electrical analyses and (b) subsequent heat transfer analyses.

Simulated Impulse Current Waveforms

The Society of Automotive Engineers (SAE) Aerospace Recommended Practice (ARP) 5412 B [35] provides standard impulse current waveforms consistent with *actual* lightning strikes (or discharge),

$$I(t) = I_0\left(e^{-\alpha t} - e^{-\beta t}\right) \quad (1)$$

where I_0 is a current constant, α is the inverse of the rise time (between 10-90% of the peak amplitude), and β is the inverse of the fall time (to decay 50% of the peak amplitude). A positive value of I_0 sets peak amplitude; α and β determine temporal characteristics of an impulse current waveform. In the 50 kA peak current impulse current waveform, I(t), employed in the FE parametric study, I_0 = 54,703 A, α = 2,278 s^{-1}, and β = 1,294,530 s^{-1}.

Matrix Decomposition Prediction Criteria

The lightning strike FE models in references [15, 16] can be used to calculate the spatially-varying local temperature and the corresponding matrix thermal decomposition caused by electrical current at each time increment during the simulations. Irreversible matrix damage (degradation) is modeled by updating the degree of matrix decomposition based on the highest temperature reached at that location. Matrix thermal decomposition was assumed to develop linearly over the temperature range 300-500˚C (i.e., between normalized values of 0 (no damage) at 300˚C and 1 (complete matrix decomposition) at 500˚C [15, 16]. The predicted matrix decomposition domains using this criteria are consistent with experimental results [36].

Damage in a sacrificial lightning protection layer may be more or less severe than damage in the underlying plies and may require standard repairs. The predicted damage in the PCFP outer layer was not considered in this study, but was considered in our earlier work [16]. One goal of

this work is to assess matrix decomposition in the outermost structural AS4/3506 ply; such plies will experience the most severe thermal damage. Since damage progressively decreases with depth below the surface [15, 16, 22, 30], outer ply damage can be used to assess the effectiveness of a given lightning protection layer.

FE Model Validation

Our previously published FE models [15, 16] were successfully validated with laboratory-scale artificial lightning strike tests [32, 33]. The FE models predicted carbon fiber ablation/sublimation and epoxy matrix decomposition based on the local temperature history. The predicted carbon fiber sublimation domain was negligible due to the relatively high sublimation temperature (≥3,300˚C), compared to epoxy matrix decomposition temperatures (typically, 300-600˚C). The time duration that the carbon fibers experience above 3,300˚C was very short and the dimensions of that very high temperature region was quite small and located near the arc attachment region, which is always the most intensively damaged region experimentally and in our predictions. Therefore, the carbon fiber sublimation region was totally encompassed by the widespread matrix damage region. The shape and size of the predicted epoxy matrix decomposition domains agreed fairly well with experimentally measured results. Figure 4 compares actual and predicted lightning damage in the outermost layer of unprotected, copper mesh (CM)-protected, and PCFP-protected similar (AS4/8552) carbon/epoxy laminates subjected to 50 kA nominal peak current.

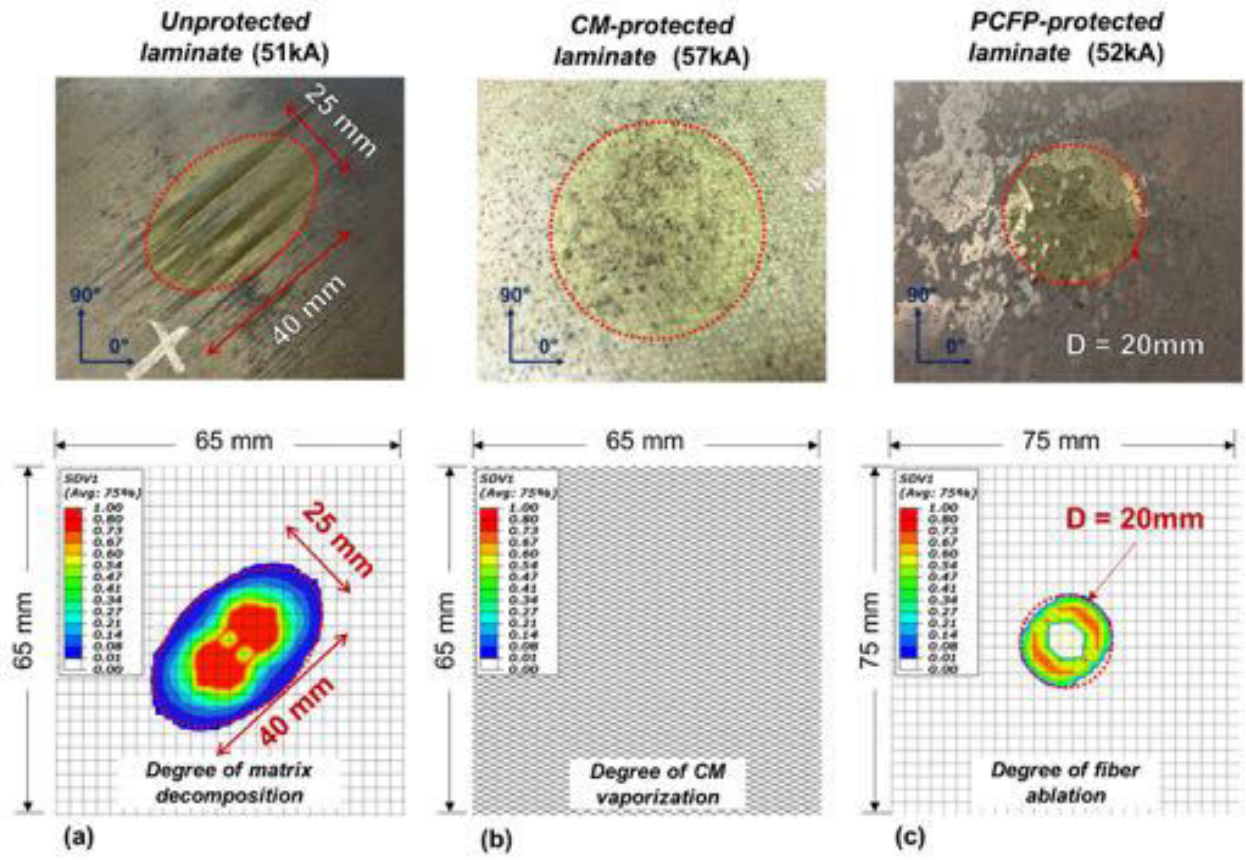

Figure 4.Comparison of actual and predicted lightning damage in the outermost layer of (a) unprotected, (b) CM-protected, and (c) PCFP-protected AS4/8552 carbon/epoxy laminates subjected to 50 kA nominal peak current: the measured peak current is included for clarity [15].

5

Predicted Epoxy Matrix Decomposition Domains

The electrical conductivities for a given protection layer play an essential role in determining the transient electrical and thermal responses of the underlying composite during a lightning strike. The use of a highly conductive *isotropic* lightning protection layer primarily distributes the

10 electrical current mostly over its surface, thus protecting the underlying composite. For a *transversely isotropic* PCFP lightning protection layer, however, the surface (electrical) current density distribution may be affected by both the in-plane and through-thickness electrical conductivities. For a given level of current, a lower through-thickness electrical conductivity yields

higher in-plane electrical currents and higher local surface current densities. The higher local current density can potentially lead to an increase in localized Joule heating.

Two-step FE simulations were performed to assess the degree of matrix decomposition in PCFP-protected AS4/3506 laminates subjected to 50 kA peak currents. Coupled electrical-thermal analyses were performed to predict the matrix damage due to Joule heating over the first 30 μs following lightning attachment. Heat transfer analyses were also performed for an additional 10 s after lightning attachment to assess matrix damage due to heat conduction in the laminate, which occurs over a much longer time scale. The degree of matrix damage in the outermost AS4/3506 ply was expressed on a scale of 0-1 (i.e., 5-100% decomposition), as described previously [15, 16].

Effect of Electrical Conductivities on Lightning Damage Development

Damage predicted in the outer +45° ply using the baseline PCFP properties for a composite subjected to a 50 kA peak current is shown in Figs. 5a and 5f. The predicted matrix decomposition in the top +45° ply 30 μs after the initial lightning attachment (i.e., at the end of the coupled electrical-thermal analysis) is shown in Fig. 5a. Matrix decomposition developed in a "figure-eight" configuration, where damage tended to elongate in the direction of the conducting carbon fibers in that ply. Two relatively small regions ("lobes") with complete matrix decomposition were located adjacent to the attachment point. Given the short time scale involved, such damage is primarily due to Joule heating. In contrast, Fig. 5f shows the additional predicted matrix decomposition due to conduction after 10 s of transient heat transfer analysis. The damaged region extended significantly in the direction perpendicular to the fibers, and became elliptical in shape. The zone with complete matrix decomposition (red) increased substantially in comparison to that associated with Joule heating. Thus, Joule heating and subsequent heat transfer contribute.

In Figs. 5b-5e, damage predicted in the outermost AS4/3506 plies after 30 μs of the coupled electrical-thermal analysis are shown for Cases 1-4, respectively, where the PCFP in-plane and through-thickness *electrical* conductivities were varied (Table 3). Note that baseline PCFP thermal conductivities and gap conductances were used. No matrix decomposition was predicted in the AS4/3506 lamina when the *in-plane* electrical conductivity of the PCFP outer layer increased by a factor of 10 (Case 1, Fig. 5b). This makes sense since a PCFP outer layer with higher in-plane electrical conductivity effectively distributes electrical current more rapidly over its surface. This, in turn, results in a lower degree of instantaneous Joule heating in the PCFP outer layer and underlying composite. In contrast, lowing the PCFP in-plane electrical conductivity by an order-of-magnitude (Case 2, Fig. 5c) resulted in increased Joule heating in the PCFP layer and more thermal damage to the underlying AS4/3506 ply.

When the *through-thickness* electrical conductivity was increased (Case 3, Fig. 5d) or reduced (Case 4, Fig. 5e) by an order-of-magnitude from the baseline values, the matrix decomposition domains in the outermost AS4/3506 ply did not appreciably change. Provided the in-plane electrical conductivity is sufficiently high, order-of-magnitude changes in the PCFP through-thickness electrical conductivity did not significantly affect matrix decomposition in the underlying composite. Figures 5g-5j show the matrix decomposition in the top AS4/3506 ply for Cases 1-4 after 10 s of subsequent transient heat transfer analysis. With the exception of Case 1 (Fig. 5g) where no matrix decomposition occurred due to Joule heating or heat conduction resulting from high PCFP in-plane electrical conductivities, the all remaining cases resulted in a significant increase in thermal damage due to heat conduction. Of course, this affect was much more pronounced for Case 2 (Fig. 5h) since the PCFP in-plane electrical conductivities were 10 times lower than that for the baseline case (Fig. 5f). Cases 1 (Figs. 5b and 5g) and 2 (Figs. 5c and

5h) clearly underscore the importance of maximizing the in-plane electrical conductivities of the protection layer in order to minimize matrix decomposition in the underlying composite. In essence, protection layers with sufficiently high in-plane electrical conductivities reduce the local electrical current densities and Joule heating in the protection layer and composite, which also leads to less transient heat conduction in the composite.

When both the PCFP in-plane and through-thickness electrical conductivities were simultaneously increased by a factor of 10 (Case 5, Figs. 6a and 6c), the predicted damage was identical to that for Case 2 (Figs. 5b and 5g), i.e., no matrix decomposition occurred in the top AS4/3506 ply. Similarly, when these properties were both reduced by an order-of-magnitude from the baseline values, the predicted matrix decomposition to the outermost AS4/3506 ply was a relative maximum (Case 6, Figs. 6b and 6d), and were virtually the same as Case 2 (Figs. 5c and 5h). These results further illustrate the importance of high PCFP in-plane electrical conductivity on minimizing thermal damage to composite structures.

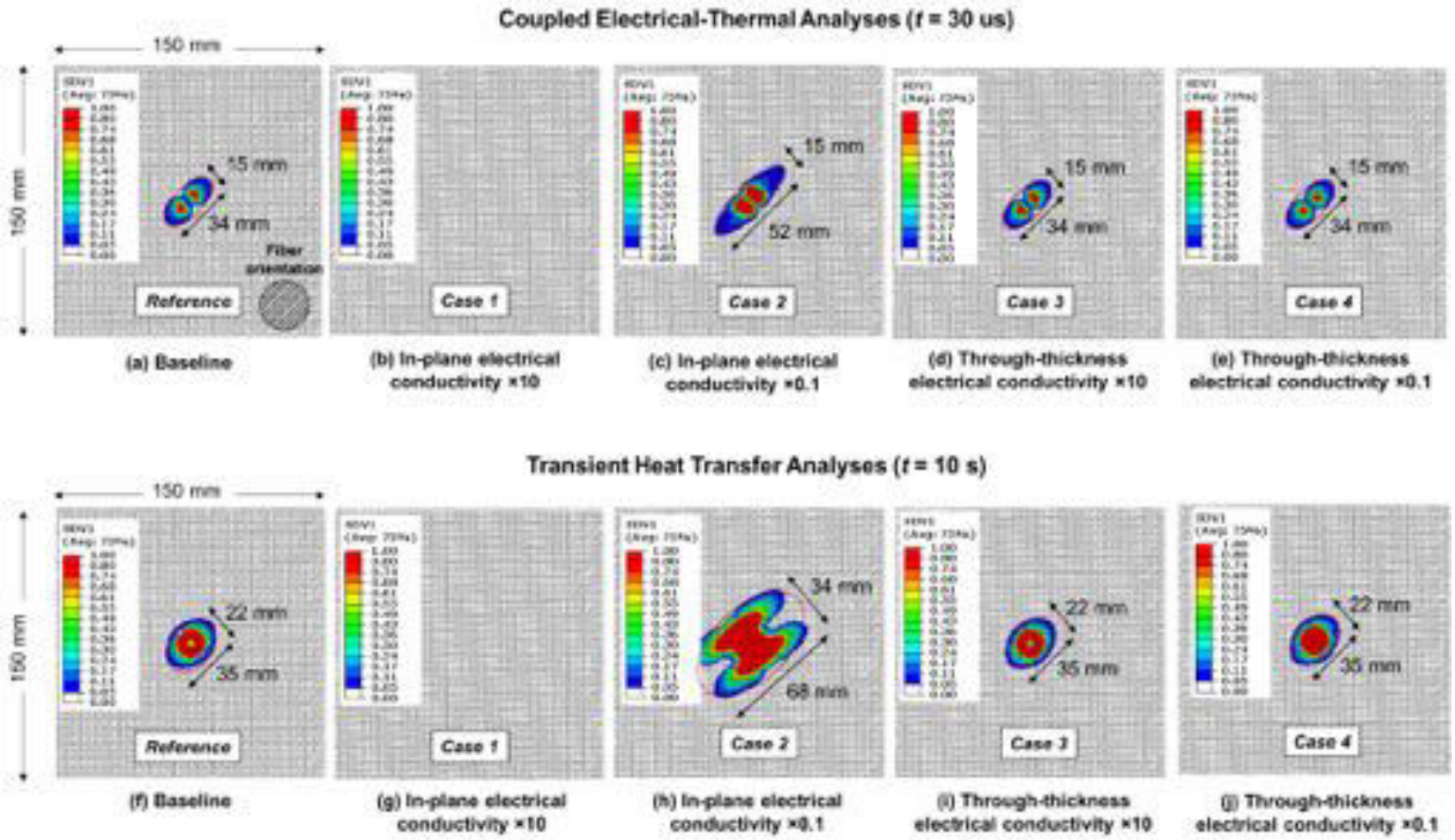

Figure 5. Predicted matrix decomposition domains in the top +45° AS4/3506 ply of PCFP-protected composites subjected to 50 kA peak currents (upper figures) after 30 μs of coupled electrical-thermal analysis and (lower figures) after 10 s of transient heat transfer analysis. Damage from various PCFP in-plane and through-thickness *electrical conductivities* are shown. Note that each figure includes the only varied PCFP in-plane and through-thickness electrical conductivities while all other properties remain the same as the baseline PCFP properties (Table 2).

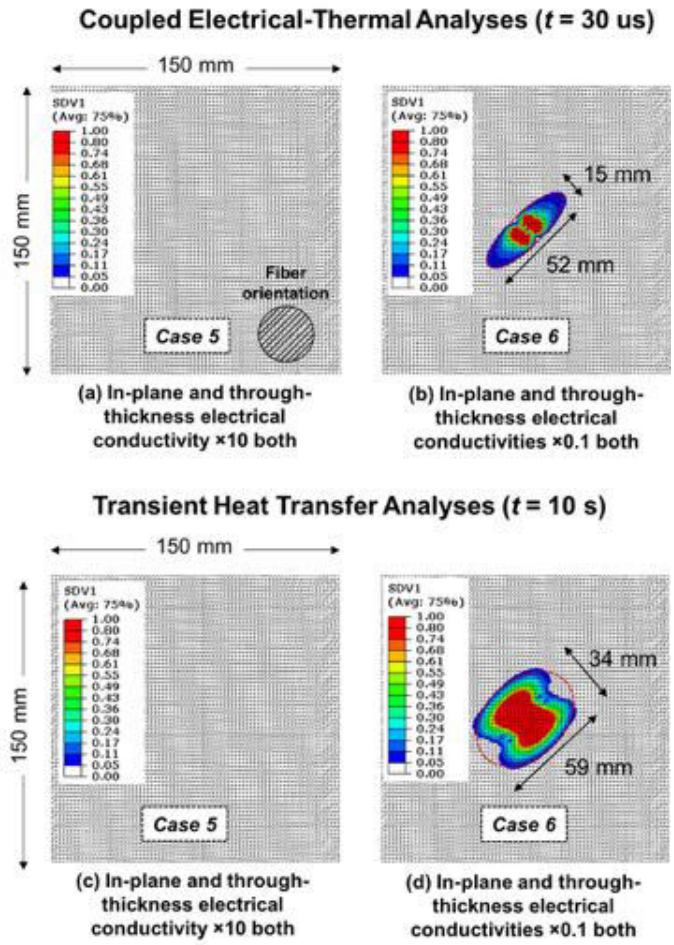

Figure 6. Predicted matrix decomposition domains in the top +45° AS4/3506 ply of PCFP-protected composites (upper images) 30 µs after being subjected to 50 kA peak currents and (lower images) after 10 s of transient heat transfer analysis. Only PCFP in-plane and through-thickness electrical conductivities are varied while all other properties remain the same as the baseline values.

Effect of Thermal Conductivities on Lightning Damage Development

Lightning is defined as a transient electrical discharge [2] that delivers large amounts of electrical energy (instantaneously dissipated as heat energy by Joule heating) to aircraft composites. In addition, dynamic mechanical pressure loads due to arc channel attachment and expansion, arc magneto-hydrodynamic effects, and internal current flow (i.e., magnetic pressure [37]) can produce significant amounts of mechanical damage [37]. Such mechanical damage is not

considered here, but is generally less widespread than thermally-induced damage [38]. Electrical current flow, current densities, Joule heating and its corresponding (nearly instantaneous) temperature rise are directly associated with composite electrical conductivities. Once (lightning) current injection is completed, composite damage may continue due to subsequent heat conduction. In general, Joule heating causes more significant instantaneous damage to composites than does the subsequent damage due to heat conduction [30, 39].

An additional set of six FE simulations of 50 kA peak current lightning strikes to PCFP-protected AS4/3506 laminates were performed (Cases 7-12, Table 3). In these simulations, the PCFP electrical conductivities, electrical gap conductance, and thermal gap conductance were held at fixed baseline values. The PCFP in-plane and through-thickness *thermal* conductivities, however, were each independently increased/decreased by one order-of-magnitude from baseline values to assess their effects on thermal damage development in the laminate (Cases 7-10, Table 3). Two additional simulations were performed where the in-plane and through-thickness thermal conductivities were *simultaneously* increased/decreased ten-fold from baseline values (Cases 11-12, Table 3). As expected in each case, the predicted matrix decomposition due to instantaneous Joule heating at the end of the coupled electrical-thermal analyses (t = 30 μs) was nearly identical to that for the baseline case (Fig. 5a). This makes sense since relatively little heat conduction can occur during the lightning attachment period of 30 μs. Interestingly, after 10 s of transient heat transfer analysis, the degree of matrix decomposition in the outmost AS4/3506 ply for each case was also nearly identical to the baseline composite (Fig. 5f). This suggests that the thermal conductivities of the relatively thin PCFP layer do not significantly affect thermal damage development in the underlying laminate. Since Joule heating in the PCFP layer is virtually instantaneous, the interface between the PCFP layer and outermost AS4/3506 ply may essentially

act like a temperature boundary condition; heat conduction *within* the PCFP may play little role on heat conduction and thermal damage in the composite. These results are consistent with the predictions available in literature [40, 41].

Effect of Gap Conductances on Lightning Damage Development

Joule heating occurring at the interface between contacted layers (due to the through-thickness current flow) is *inversely* proportional to the electrical gap conductance [7]. A higher electrical gap conductance between the PCFP protection layer and AS4/3506 laminate may cause less Joule heating per unit current flow, leading to potentially less thermal damage in the AS4/3506 plies. In contrast, the through-thickness heat conduction at an interface between contacted layers is proportional to the thermal gap conductance [7]. The greater the thermal gap conductance, the more heat is transferred through an interface. Therefore, a lower thermal gap conductance between the PCFP protection layer and composite may lead to reduced thermal damage in the underlying laminate.

A final set of four 50 kA peak current lightning strike simulations were performed where the electrical and thermal *gap conductances* between the PCFP protection layer and AS4/3506 composite were each independently increased/decreased by one order-of-magnitude from the conductivities were held fixed in the simulations. Figure 5 contains a plot of the predicted matrix decomposition at the end of Joule heating (t = 30 μs) and transient heat conduction analyses (t = 10 s) for each case. For example, Case 13 (Figs. 7a and 7e) and Case 14 (Figs. 7b and 7f) correspond to analyses where the electrical gap conductances were increased/decreased ten-fold, respectively from the baseline values. In both cases, the predicted matrix decomposition was indistinguishable from the baseline case (Figs 5a and 5f). Hence, for the intermediate peak current

(i.e., 50 kA) and range of electrical properties considered, composite matrix decomposition is relatively insensitive to changes in both through-thickness electrical conductivities (Fig. 4) and changes in the electrical gap conductances between the protection layer and laminates (Figs. 7a and 7b). In essence, the PCFP layer may be too thin for the given variations in through-thickness electrical conductivities to appreciably affect through-thickness current flow. Likewise, the gap between the PCFP and underlying composite may be insufficient to be a significant electrically isolating element over the range of resistance values considered.

Analogously, in Case 15 (Figs. 7c and 7g) and Case 16 (Figs. 7f and 7h), the thermal gap conductance was increased/decreased ten-fold, respectively, from its baseline values. Not surprisingly, at the end of Joule heating (t = 30 μs), the predicted matrix decomposition for the case of increased (Fig. 7c) or decreased (Fig. 7d) thermal gap conductance was nearly the same as the baseline case (Fig. 5a) (i.e., not enough time had transpired for significant heat conduction to occur across the PCFP/laminate interface). At the end of the transient heat transfer analyses (t = 10 s), the predicted size and intensity of the matrix decomposition region associated with a ten-fold *increase* in thermal gap conductance (Fig. 7g) were consistent with those for the baseline case (Fig. 5f). Perhaps for the given intermediate peak current, local temperature distributions, and heat fluxes, the baseline gap properties reasonably approximate perfect interface. When the thermal gap conductance was decreased by an order-of-magnitude, however, the size of the matrix decomposition domain (Fig. 7h) decreased by roughly 10% relative to the baseline case (Fig. 5d). This suggests that the interfacial thermal properties between the protection layer and composite may be tailored in order to achieve modest improvement in protection system performance.

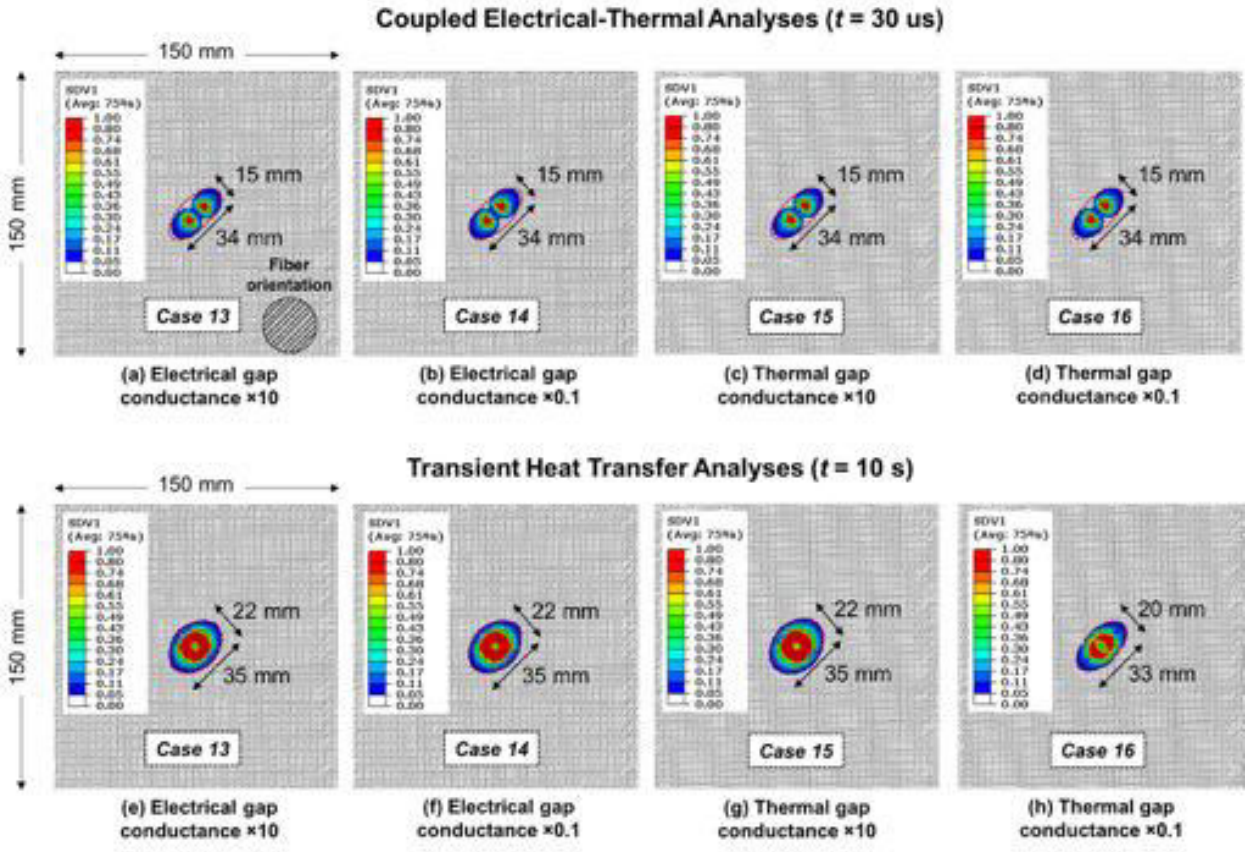

Figure 7. Predicted matrix decomposition domains in the top +45° AS4/3506 ply of PCFP-protected composites subjected to 50 kA peak currents at the end of coupled electrical-thermal analyses (upper images) and transient heat transfer analyses (lower images). Damage is shown using various PCFP electrical and thermal gap conductances.

Effect of PCFP Properties on the Through-Thickness Damage to AS4/3506 Laminates

The preceding 17 numerical simulations were used to assess the through-thickness thermal damage penetration (defined as the maximum depth containing matrix decomposition) of PCFP-protected 9-ply AS4/3506 laminates subjected to a 50 kA peak current. The predicted matrix damage obtained using the baseline PCFP properties (Table 2) penetrated the first three plies (i.e., 0.6 mm). Table 4 contains a summary of the number of damaged AS4/3506 plies and total depth of damage penetration for each of the 16 cases considered in the parametric study. Based upon the parametric study, the size, intensity, and depth of penetration of matrix thermal

decomposition was driven by the value of the PCFP in-plane electrical conductivity. When the baseline protection layer in-plane electrical conductivity was employed (Cases 3, 4, and 6-16, Table 4), matrix decomposition penetrated through one-third of the laminate, irrespective of order-of-magnitude changes in PCFP through-thickness electrical conductivity, thermal conductivities, and electrical/thermal gap conductances. Moreover, the size and intensity of the matrix decomposition domain in each ply was essentially the same as for the baseline case (with the exception of a minor reduction in damage size associated with a decrease in thermal gap conductance, Case 16). For the two analyses where the PCFP in-plane electrical conductivity was 10 times greater than the baseline value (Cases 1 and 5), *no* matrix thermal damage was predicted (Table 4, Figs. 5-6). Conversely, a ten-fold decrease in PCFP in-plane electrical conductivity (Cases 2 and 6) led to maximal damage in the outermost ply (Figs. 5h and 5d) and a total penetration depth of penetration of five plies (Table 4). Clearly, maximizing the in-plane electrical conductivity of the protection layer is of paramount importance in reducing underlying thermal damage to composite structures.

Table 4. Predicted maximum damage penetration depths of 9-ply PCFP-protected AS4/3506 composites [+45/-45/0_2/90/0_2/-45/+45] subjected to 50 kA peak currents

Simulation	Number of damaged plies	Max. penetration depth[a] (mm)	Simulation	Number of damaged plies	Max. penetration depth[a] (mm)
Case 1	0	0.0	Case 9	3	0.6
Case 2	5	1.0	Case 10	3	0.6
Case 3	3	0.6	Case 11	3	0.6
Case 4	3	0.6	Case 12	3	0.6
Case 5	0	0.0	Case 13	3	0.6
Case 6	5	1.0	Case 14	3	0.6
Case 7	3	0.6	Case 15	3	0.6
Case 8	3	0.6	Case 16	3	0.6

[a]Maximum penetration depth is calculated by multiplying the number of damaged layers by the ply thickness (0.2 mm). The predicted damage penetration obtained from baseline PCFP properties (Case 0) was the third layer (i.e., 0.6 mm).

The significance of PCFP properties on thermal damage development may be more noticeable at higher peak currents due to increased Joule heating. Three additional FE simulations were conducted using 200 kA peak current lightning strikes to PCFP-protected 9-ply AS4/3506 laminates. In the first simulation, the baseline PCFP properties were used. In the latter two simulations, the PCFP in-plane electrical conductivity was increased one and two orders-of-magnitude from the baseline value. For comparison purposes, a typical copper protection layer has an electrical conductivity 300 (at 1,000˚C) and 5000 times (at 20˚C) greater than the in-plane baseline PCFP property considered in this study [42]. Figure 6 shows the predicted matrix decomposition and corresponding through-thickness damage penetration of the three PCFP-protected AS4/3506 laminates subjected to 200 kA peak currents at the end of heat transfer analyses (t = 10 s). When the baseline PCFP properties (Table 2) were employed in the FE model, the matrix decomposition in the top AS4/3506 ply (Fig. 8a) was far more severe than that obtained from a 50 kA peak current (Fig. 5f). The size of the damage in the outermost +45˚ ply was roughly

four times larger than for a 50 kA strike and the complete thermal decomposition damage (i.e., red region) penetrated through all nine underlying plies. In contrast, PCFP outer layers designed with in-plane electrical conductivities 10x (Fig. 8b) and 100x (Fig. 8c) greater than the baseline value markedly reduced or completely eliminated matrix decomposition, respectively, resulting from a 200 kA strike. In the former case, a minor amount of matrix decomposition was predicted, but was limited to the outermost AS4/3506 ply (Fig. 8b). As an aside, the 200 kA peak current is the maximum current specified in SAE ARP 5412 B [35].

In practice, the PCFP in-plane electrical conductivities can be improved by tailoring the fiber volume fraction and orientation. Alternatively, PCFP can be doped with tiny amounts of highly conductive metallic nanoparticles or coated with such metals to dramatically increase a protection layer's electrical conductivities without appreciably affecting its mass. Doping may also prove useful in enhancing the electrical/thermal conductivities of the adhesive layer between the protection layer and composite, as well as increasing the conductivities in the outermost composite plies adjacent to the protection layer. Use of conductive adhesives and resins may also lead to improvements in lightning damage resistance. The PCFP represents only one potential carbon-based protection layer. Use of lightweight, thin graphene papers containing exceptionally conductive (in 2-D versus 1-D for nanofibers), high strength, aligned graphene/graphite nanoplatelets may provide an attractive alternative to traditional metallic protection layers. Such options are currently under investigation at Mississippi State University. In addition, through transmission ultrasonic testing combined with destructive sectioning of actual lightning strike test panels is currently underway to clearly understand through-thickness damage development in AS4/3506 composites underneath a PCFP outer layer. This will be discussed in a subsequent publication.

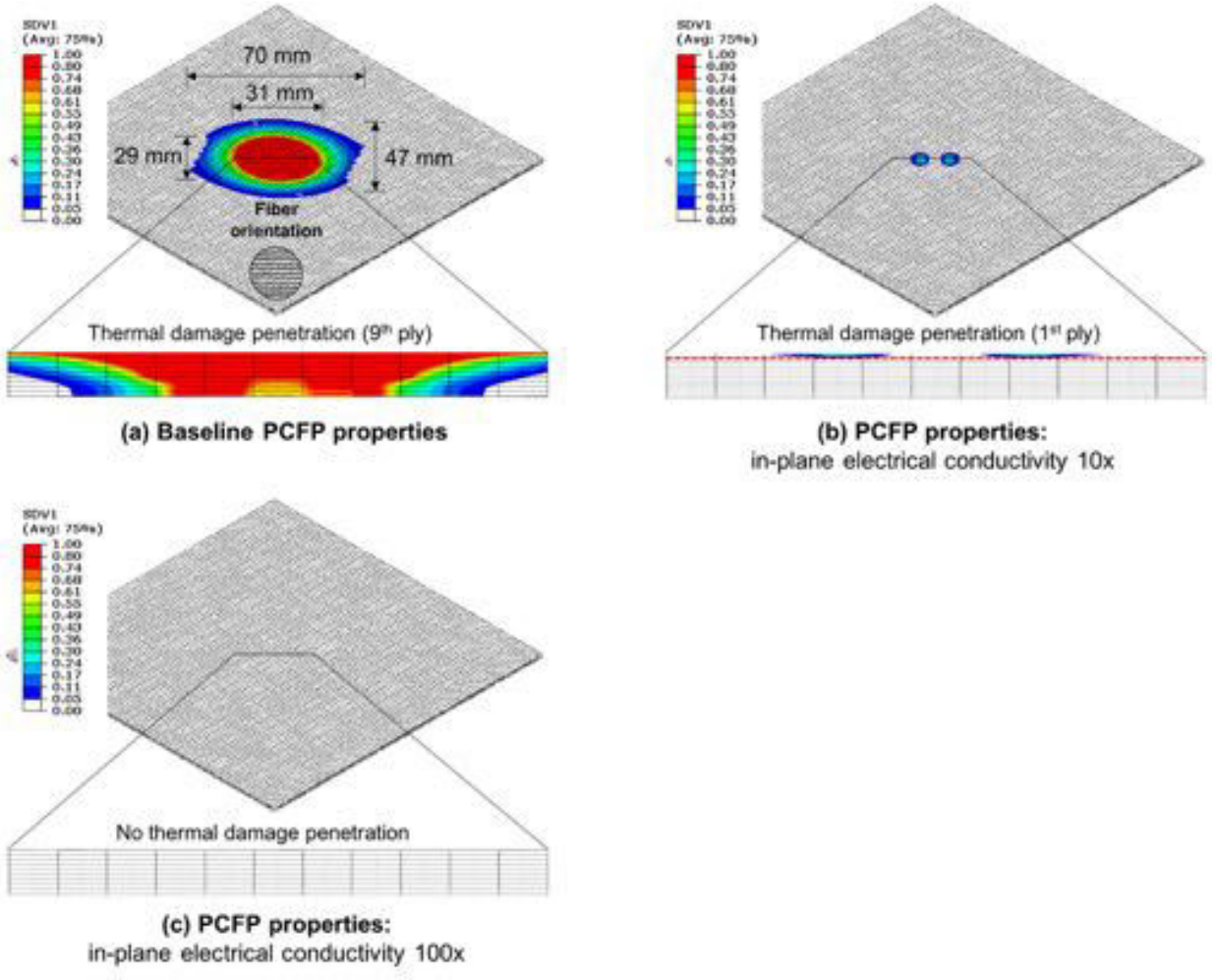

Figure 8. Matrix thermal decomposition and corresponding damage penetration in PCFP-protected 9-ply AS4/3506 laminates subjected to 200 kA peak currents after 10 s of transient heat transfer analyses. PCFP protection layers designed with (a) baseline in-plane electrical conductivities, (b) 10x, and (c) 100x greater than the baseline values.

Concluding Remarks

A parametric study investigated non-metallic lightning protection layer properties that lead to thermal damage mitigation in the underlying composite structure. Pitch-based carbon fiber paper (PCFP)-protected AS4/3506 carbon/epoxy laminates subjected to 50 kA and 200 kA peak currents were considered. The lightning protection characteristics of various PCFP outer layers were

compared by varying in-plane and through-thickness properties: *i*) electrical conductivity, *ii*) thermal conductivity, *iii*) electrical gap conductance, and *iv*) thermal gap conductance.

PCFP in-plane electrical conductivity is the essential factor in reducing lightning-induced thermal damage development. The predicted epoxy matrix decomposition in the underlying AS4/3506 plies significantly decreased as the PCFP in-plane electrical conductivity increased. The effect of PCFP through-thickness electrical conductivity and electrical gap conductance on the matrix thermal decomposition were negligible. While predicted matrix thermal damage decreased slightly with a decrease in thermal gap conductance, varying the electrical gap conductance and the in-plane and through-thickness thermal conductivities did not significantly affect lightning thermal damage development. This FE parametric study clearly shows the importance of maximizing the in-plane electrical conductivities of the protection layer in order to minimize matrix decomposition in the underlying composite and suggests how to tailor non-metallic lightning protection layers as an alternative to traditional isotropic metallic protection layers.

References

1. Baker, A., Dutton, S., and Kelly, D., *Composite Materials for Aircraft Structures*. AIAA Education Series. 2004: AIAA.
2. Uman, M., and Rakov, V., *The Interaction of Lightning with Airborne Vehicles.* Progress in Aerospace Sciences, 2003. **39**(1): p. 61-81.
3. Plumer, J.A., and Hourihan, B.I. *Data from the Airlines Lightning Strike Reporting Project*. in *In Proceedings of the Lightning and Static Electricity Conference*. 1972.
4. Fisher, F.A., and Plumer, J.A., *Lightning Protection of Aircraft.* 1977.
5. McDowall, R.L., Plumer, J.A., and Glynn, M.S. *Lightning Data Acquisition*. in *Proceedings of the 15th International Aerospace and Ground Conference on Lightning and Static Electricit*. 1992. Atlantic City, NJ.
6. O'Loughlin, J.B., and Skinner, S.R., *General Aviation Lightning Strike Report and Protection Level Study*. 2004, DOT/FAA/AR-04/13, FAA.
7. Ohm, G.S., *Die galvanische Kette, Mathematisch Bearbeitet*. 1827: Riemann.
8. Bazelyan, E.M., and Raizer, Y.P., *Lightning Physics and Lightning Protection*. 2000: CRC Press.

9. Sweers, G., B. Birch, and J. Gokcen, *Lightning Strikes: Protection, Inspection, and Repair.* AERO Quarterly. GTR, 2004. **12**: p. 19-28.
10. Gagné, M., and Therriault, D., *Lightning Strike Protection of Composites.* Progress in Aerospace Sciences, 2014. **64**: p. 1-16.
11. Hirano, Y., Yokozeki, T., Ishida, Y., Goto, T., Takahashi, T., Qian, D., Ito, S., Ogasawara, T., and Ishibashi, M., *Lightning Damage Suppression in a Carbon Fiber-Reinforced Polymer with a Polyaniline-based Conductive Thermoset Matrix.* Composites Science and Technology, 2016. **127**: p. 1-7.
12. Gou, J., Tang, Y., Liang, F., Zhao, Z., Firsich, D., and Fielding, J., *Carbon Nanofiber Paper for Lightning Strike Protection of Composite Materials.* Composites Part B: Engineering, 2010. **41**(2): p. 192-198.
13. Wang, S., R. Downes, C. Young, D. Haldane, A. Hao, R. Liang, B. Wang, C. Zhang, and R. Maskell, *Carbon Fiber/Carbon Nanotube Buckypaper Interply Hybrid Composites: Manufacturing Process and Tensile Properties.* Advanced Engineering Materials, 2015. **17**(10): p. 1442-1453.
14. Han, J., Zhang, H., Chen, M., Wang, D., Liu, Q., Wu, Q., and Zhang, Z., *The Combination of Carbon Nanotube Buckypaper and Insulating Adhesive for Lightning Strike Protection of the Carbon Fiber/Epoxy Laminates.* Carbon, 2015. **94**: p. 101-113.
15. Lee, J., Lacy, T.E., Pittman, Jr., C.U., and Mazzola, M.S., *Thermal Response of Carbon Fiber Epoxy Composites with Metallic and Nonmetallic Protection Layers to Simulated Lightning Currents.* Polymer Composites, 2017.
16. Lee, J., Lacy, T.E., Pittman, Jr., C.U., and Mazzola, M.S., *Temperature-Dependent Thermal Decomposition of Carbon/Epoxy Laminates Subjected to Simulated Lightning Currents.* Polymer Composites, 2017.
17. Fu, K., Ye, L., Chang, L., Yang, C., and Zhang, Z, *Modelling of Lightning Strike Damage to CFRP Composites with an Advanced Protection System. Part I: Thermal–Electrical Transition.* Composite Structures, 2017.
18. Menousek, J.F., and Monin, D.L., *Laser Thermal Modeling of Graphite Epoxy.* Naval Weapons Center Technical Memorandum, 1979. **3834**.
19. Mueller, G., *Simulation of Repetitively-Pulsed Laser Irradiation of Graphite-Epoxy Composite*. 1984, DTIC Document (NRL-MR-5467), Naval Research Laboratory: Washington DC.
20. Griffis, C.A., Nemes, J.A., Stonesifer, F.R., and Chang, C.I., *Degradation in Strength of Laminated Composites Subjected to Intense Heating and Mechanical Loading.* Journal of Composite Materials, 1986. **20**(3): p. 216-235.
21. Fanucci, J.P., *Thermal Response of Radiantly Heated Kevlar and Graphite/Epoxy Composites.* Journal of Composite Materials, 1987. **21**(2): p. 129-139.
22. Abdelal, G., and Murphy, A., *Nonlinear Numerical Modelling of Lightning Strike Effect on Composite Panels with Temperature Dependent Material Properties.* Composite Structures, 2014. **109**: p. 268-278.
23. Suzuki, Y., Todoroki, A., Matsuzaki, R., and Mizutani, Y., *Impact-Damage Visualization in CFRP by Resistive Heating: Development of a New Detection Method for Indentations Caused by Impact Loads.* Composites Part A: Applied Science and Manufacturing, 2012. **43**(1): p. 53-64.

24. Raffray, R. *Assessment of Dry Chamber Wall Configurations as Preliminary Step in Defining Key Processes for Chamber Clearing Code*. 2001 [cited 2015 17 Jun]; Available from: http://aries.ucsd.edu/raffray/presentations/HAPL/HAPL_May01_ARR.pdf.
25. Osaka Gas Chemicals. *DONACARBO Paper Data Sheet*. [cited 2015 17 Jun]; Available from: http://www.ogc.co.jp/e/products/carbon-f/donacarbo_paper.html.
26. Potts, R.L., *Application of integral methods to ablation charring erosion-A review.* Journal of Spacecraft and Rockets, 1995. **32**(2): p. 200-209.
27. Wang, S. and D. Chung, *Electrical Behavior of Carbon Fiber Polymer-Matrix Composites in the Through-Thickness Direction.* Journal of Materials Science, 2000. **35**(1): p. 91-100.
28. Pradère, C., Batsale, J.C., Goyhénèche, J.M., Pailler, R., and Dilhaire, S., *Thermal Properties of Carbon Fibers at Very High Temperature.* Carbon, 2009. **47**(3): p. 737-743.
29. Mirmira, S., M. Jackson, and L. Fletcher, *Effective Thermal Conductivity and Thermal Contact Conductance of Graphite Fiber Composites.* Journal of Thermophysics and Heat transfer, 2001. **15**(1): p. 18-26.
30. Ogasawara, T., Y. Hirano, and A. Yoshimura, *Coupled Thermal–Electrical Analysis for Carbon Fiber/Epoxy Composites Exposed to Simulated Lightning Current.* Composites Part A: Applied Science and Manufacturing, 2010. **41**(8): p. 973-981.
31. ABAQUS, *ABAQUS Documentation.* Dassault Systémes Simulia Corp., 2014.
32. Lacy, T.E., Mazzola, M.S., Lee, J., Gharghabi, P., Boushab, D., and Ricks, T.M., *Lightning Strike Testing on PRSEUS Panels*, in *Boeing Technical Report (Yr 2016-2017)*.
33. Lacy, T.E., Mazzola, M.S., Kluss, J., Boushab, D., Gharghabi, P., Lee, J., and Ricks, T.M., *Lightning Strike Testing on PRSEUS Panels*, in *Boeing Technical Report (Yr 2017-2018)*.
34. Jiang, P., Zhao, C., Deng, J., and Zhang, W. *Experimental Investigation of Local Heat Transfer of Carbon Dioxide at Super-Critical Pressures in a Vertical Tube and Multi-Port Mini-Channels Under Cooling Conditions*. in *International Refrigeration and Air Conditioning Conference at West Lafayette, IN, July 14-17*. 2008.
35. SAE, *Aircraft Lightning Environment and Related Test Waveforms.* Aerospace Recommended Practice ARP 5412, 1999.
36. Hirano, Y., Katsumata, S., Iwahori, Y., and Todoroki, A., *Artificial Lightning Testing on Graphite/Epoxy Composite Laminate.* Composites Part A: Applied Science and Manufacturing, 2010. **41**(10): p. 1461-1470.
37. Chemartin, L., P. Lalande, B. Peyrou, A. Chazottes, P. Elias, C. Delalondre, B. Cheron, and F. Lago, *Direct Effects of Lightning on Aircraft Structure: Analysis of the Thermal, Electrical and Mechanical Constraints.* AerospaceLab, 2012(5): p. 1-15.
38. Foster, P., Abdelal, G, and Murphy, A, *Quantifying the Influence of Lightning Strike Pressure Loading on Composite Specimen Damage.* Applied Composite Materials, 2018: p. 1-23.
39. Lee, J., Lacy, T.E., Pittman, Jr., C.U. & Mazzola, M.S. *Thermal Response to Simulated Lightning Currents on Stitched Composite Aircraft Structures*. in *Proceedings of the American Society for Composites: 31st Technical Conference, Williamsburg, VA, Sep 19-21*. 2016.
40. Wang, F.S., Ding, N., Liu, Z.Q., Ji, Y.Y., and Yue, Z.F., *Ablation Damage Characteristic and Residual Strength Prediction of Carbon Fiber/Epoxy Composite Suffered from Lightning Strike.* Composite Structures, 2014. **117**: p. 222-233.

41. Dong, Q., Guo, Y., Chen, J., Yao, X., Yi, X., Ping, L., and Jia, Y., *Influencing Factor Analysis based on Electrical-Thermal-Pyrolytic Simulation of Carbon Fiber Composites Lightning Damage.* Composite Structures, 2016. **140**: p. 1-10.
42. Gathers, G., *Thermophysical Properties of Liquid Copper and Aluminum.* International Journal of Thermophysics, 1983. **4**(3): p. 209-226.